

Syntheses and Crystal Structures of Highly Diastereomerically Enriched Lithiated Benzylsilanes in the Presence of External Donor Molecules: Experiment and Theory

Carsten Strohmann,^{*,[a]} Daniel H. M. Buchold,^[a] Timo Seibel,^[a] Kerstin Wild,^[a] and Daniel Schildbach^[a]

In memory of Ron Snaith

Keywords: Silanes / Lithium / Diastereomers / Quantum-chemical calculations / Stereochemistry

The solid-state structures of the lithiated (aminomethyl)benzylsilanes $\text{Me}_2\text{Si}[(R)\text{-(CHPhLi}\cdot 0.5\text{TMEDA)}](\text{CH}_2\text{SMP})$ [$((R,S)\text{-2})_2\cdot\text{TMEDA}$] and $\text{Me}_2\text{Si}[(R)\text{-(CHPhLi}\cdot\text{DABCO)}](\text{CH}_2\text{SMP})$ [$(R,S)\text{-2}\cdot\text{DABCO}$] [$\text{CH}_2\text{SMP} = (S)\text{-2-(methoxymethyl)pyrrolidinomethyl}$] and the absolute configurations at the stereogenic metallated carbon centres of these compounds were determined by single-crystal X-ray diffraction methods. The crystal structures of the TMEDA-bridged dimer [$(R,S)\text{-2}$] $_2\cdot\text{TMEDA}$ and monomeric $(R,S)\text{-2}\cdot\text{DABCO}$ were compared to that of the parent compound $(R,S)\text{-2}$, a coordination polymer. By computational methods [B3LYP/6-31+G(d)], the

mechanism of the deprotonation of the starting compound, (aminomethyl)benzylsilane [$(S)\text{-1}$], as well as the stability of configuration of the lithiated derivatives of $(R,S)\text{-2}$, were examined. For the highly diastereoselective substitution reactions of the derivatives of $(R,S)\text{-2}$ with iodomethane, inversion of the configuration at the metallated carbon centre was observed and correlated with the results of the quantum-chemical studies.

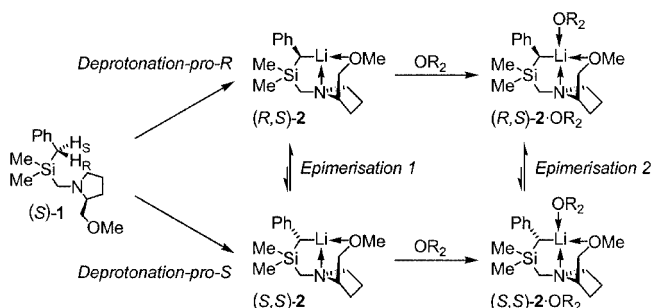
(© Wiley-VCH Verlag GmbH & Co. KGaA, 69451 Weinheim, Germany, 2003)

Introduction

The synthesis of enantiomerically or diastereomerically enriched^[1] alkyllithium compounds, in which the metallated carbon centre is the stereogenic centre, has been intensively studied for the last 20 years.^[2] Among these compounds are several enantiomerically enriched benzyl lithium reagents.^[2–5] Stereogenic metallated carbon centres are usually generated by deprotonation using alkyllithium bases, like *tert*-butyllithium. The stereochemical information can be introduced *prior* to the deprotonation reaction by using enantiomerically enriched C–H acidic precursors bearing only one proton at the stereogenic carbon centre. In contrast, methods for the introduction of the stereochemical information *during* the deprotonation reaction are either *intermolecular* by chiral auxiliaries, like (–)-sparteine, or *intramolecular* by the side-arm donation of chiral substituents, like the $(S)\text{-2-(methoxymethyl)pyrrolidinomethyl}$ substituent (CH_2SMP). This latter method is used in our laboratory.

Two different reaction conditions for the synthesis of the studied diastereomerically enriched benzyl lithium com-

pounds are applicable. *Kinetically controlled synthesis:* Diastereotopos-differentiating deprotonation at low temperatures, mostly observed in non-polar solvents (e.g. in toluene, *n*-pentane); *Thermodynamically controlled synthesis:* Epimerisation between two diastereomeric alkyllithiums at higher temperatures, mostly observed in polar solvents (e.g. in THF) (Scheme 1). Kinetically controlled deprotonation and thermodynamically controlled epimerisation will be discussed in detail in the section “Quantum-Chemical Studies”.



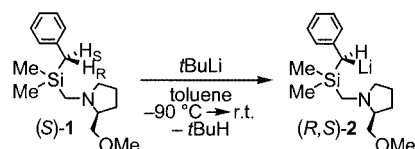
Scheme 1. Relevant deprotonation reactions and epimerisation equilibria starting from $(S)\text{-1}$

^[a] Institut für Anorganische Chemie der Universität Würzburg
Am Hubland, 97074 Würzburg, Germany
Fax: (internat.) +49-(0)931/888-4605
E-mail: mail@carsten-strohmann.de

The focus of this article will be particularly on the lithiated (aminomethyl)benzylsilane (*R,S*)-**2** in the presence of external coordinating donor molecules. The synthesis, the stability of configuration at the metallated carbon centre and further transformations (stereochemical course) have been investigated thoroughly.

The lithiation of [(benzyltrimethylsilyl)methyl]-(*S*)-**2**-(methoxymethyl)pyrrolidine [(*S*)-**1**] with *sec*-butyllithium in THF and selective substitution reactions with alkyl halides, which showed very high diastereomeric ratios (*dr*), were first reported by Chan and co-workers.^[4a] A significant solvent effect on the diastereomeric ratios of the transformations with iodomethane was observed when the reaction was carried out in THF (*dr* = 75:25) and diethyl ether (*dr* ≥ 98:2). Thus, it was of great interest to determine the solid-state structure (and the absolute configuration) of lithiated organosilane (*R,S*)-**2** in the crystal,^[6] especially since only very few enantiomerically pure alkylolithiums have been investigated in the solid state up to now.^[2a,3d,3g,7–9]

The lithiation of (aminomethyl)benzylsilane [(*S*)-**1**] was carried out with *tert*-butyllithium at –90 °C in a toluene/*n*-pentane mixture (Scheme 2). At –30 °C, yellow needles of the metallated product (*R,S*)-**2** could be isolated as single crystals in 80% yield. The result of the single-crystal X-ray diffraction study is shown in Figure 1.^[6]



Scheme 2

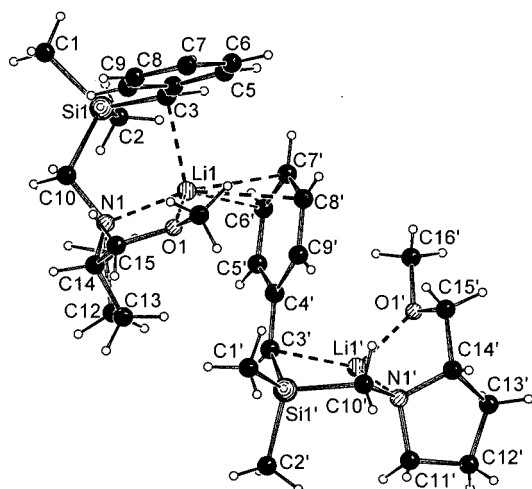
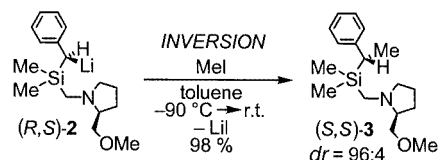


Figure 1. Molecular structure and numbering scheme of compound (*R,S*)-**2** in the crystal (Schakal plot);^[10] selected bond lengths (Å) and angles (°): Si(1)–C(3) 1.797(7), Li(1)–C(3) 2.269(14), C(3)–C(4) 1.419(9), N(1)–Li(1) 2.183(12); C(3)–Si(1)–C(10) 107.9(3)

For the substitution reaction of (*R,S*)-**2** with iodomethane in toluene/*n*-pentane, inversion of the configuration

at the metallated carbon centre was observed with a high diastereoselectivity (*dr* = 96:4). The absolute configuration of methylated (aminomethyl)benzylsilane (*S,S*)-**3** was determined by X-ray structural analysis of the corresponding ammonium iodide (Scheme 3).^[6]



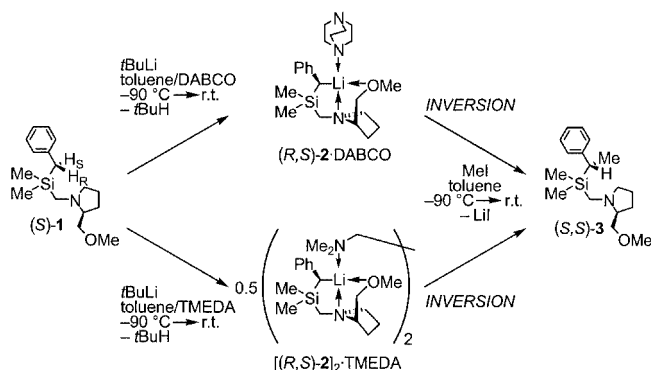
Scheme 3

Due to the difference in the stereoselectivities of the mentioned substitution reactions, when switching from non-polar solvents to polar solvents, the molecular structures of (*R,S*)-**2** with external (intermolecularly) coordinating molecules, blocking a potential vacant coordination site at the lithium centre, were to be examined. Therefore, the solid-state molecular structures of the two donor-stabilised adducts (*R,S*)-**2**·DABCO and [(*R,S*)-**2**]₂·TMEDA are presented, as well as the results of substitution reactions with the electrophile iodomethane. The stereochemical aspects of these transformations will be explained by quantum-chemical studies.

Results and Discussion

Synthesis of the Diastereomerically Enriched Alkylolithiums

[(*R,S*)-**2**]₂·TMEDA and (*R,S*)-**2**·DABCO were generated by lithiation with *tert*-butyllithium in a toluene/*n*-pentane mixture in the presence of the corresponding diamine ligand at low temperatures. After warming to room temperature, single crystals of both compounds were obtained that were suitable for X-ray structural analysis. According to this, a monomeric molecular structure was observed for (*R,S*)-**2**·DABCO, with only one nitrogen centre coordinating to one lithium centre, while a dimeric structure was determined for [(*R,S*)-**2**]₂·TMEDA with the diamine in a bridging mode [both molecular structures, with an (*R*) configuration at the lithiated carbon centre, will be discussed]. The bridged dimer [(*R,S*)-**2**]₂·TMEDA is formed indepen-



Scheme 4

dently of the molar ratio between the alkyllithium compound and TMEDA (1:1 or 2:1), and the use of half an equivalent of DABCO (molar ratio of 2:1) does not force this ligand into a bridging position (Scheme 4).

After dissolving the solids of [(*R,S*)-2]₂·TMEDA and (*R,S*)-2·DABCO in toluene, the trapping reactions with iodomethane were carried out at –90 °C and the reaction mixture was subsequently warmed to room temperature. Methylated silane (*S,S*)-3/(*R,S*)-3 was formed in maximum yields of 98%. Higher diastereomeric ratios were observed when the substitution reactions with iodomethane were carried out in the coordinating solvent diethyl ether (*dr* > 98:2), than for the corresponding reactions in a toluene/*n*-pentane mixture (*dr* = 96:4). Surprisingly, THF as a solvent gave only poor diastereomeric ratios (*dr* = 75:25).^[4a,6] Unfortunately, no single-crystals of (*R,S*)-2 from the two ethereal solvents have been obtained up to now. Thus, the absolute configurations at the lithiated carbon centres of compounds of the formal type (*R,S*)-2·OR₂ (OR₂ = THF, Et₂O) have not been confirmed for these two solvents. Due to the difference in the stereoselectivities of the substitution reaction with iodomethane in the two ethereal solvents, different reaction conditions for the methylation were applied and the diastereomeric ratios studied. The results are summarised in Table 1.

Table 1. Diastereoselectivities of substitution reactions with iodomethane in different solvents

Compound	Solvent	<i>dr</i> [(<i>S,S</i>)-3:(<i>R,S</i>)-3]
[(<i>R,S</i>)-2] ₂ ·TMEDA	toluene	>98:2
(<i>R,S</i>)-2·DABCO	toluene	>98:2
(<i>R,S</i>)-2	toluene +1 equiv. THF before metallation	>98:2
(<i>R,S</i>)-2	toluene +1 equiv. THF after metallation	>98:2
(<i>R,S</i>)-2	Et ₂ O	>98:2
[(<i>R,S</i>)-2] ₂ ·TMEDA	THF	69:31
(<i>R,S</i>)-2·DABCO	THF	62:38
(<i>R,S</i>)-2	THF	75:25

For the reactions of the defined donor adducts [(*R,S*)-2]₂·TMEDA and (*R,S*)-2·DABCO as well as for reactions where the external donor molecule is added stoichiometrically (THF), high diastereoselectivities were observed. In contrast to the methylation in the solvent diethyl ether, methylations of (*R,S*)-2, [(*R,S*)-2]₂·TMEDA and (*R,S*)-2·DABCO in THF as a solvent give only poor diastereoselectivities. Obviously, the high selectivities of reactions of (*R,S*)-2 are only diminished by the highly polar environment of THF as a solvent, while reactions of defined mixtures/adducts of (*R,S*)-2 with external coordinating donor molecules in less or non-polar solution give high diastereomeric ratios. Moreover, the stereochemical course of the transformations with the lithiated (aminomethyl)benzylsilanes is not affected by crystallisation and isolation of these compounds; reactions starting with the lithium compound as prepared and maintained in solution gave the same *dr* values.

Discussion of the X-ray Structural Analyses of [(*R,S*)-2]₂·TMEDA and (*R,S*)-2·DABCO

The alkyllithium compound [(*R,S*)-2]₂·TMEDA crystallised from a toluene/*n*-pentane mixture in the orthorhombic crystal system, space group *P*2₁2₁2₁ (see also Table 2). The asymmetric unit of [(*R,S*)-2]₂·TMEDA contains one molecule, representing a TMEDA-bridged dimer, where each nitrogen centre of the bidentate diamine ligand coordinates to one lithium centre of a silane unit (Figure 2). (Due to the similarity of the structural parameters of these two bridged silane units, only one unit is discussed; selected bond lengths are given in Table 3).

The lithium centre, with a distorted tetrahedral coordination sphere, has contacts to the metallated carbon centre C(3), to the oxygen centre O(1) and the nitrogen centre N(1) of the SMP substituent, as well as to N(3) of the TMEDA ligand. The metallated carbon centre C(3) is slightly pyramidalised: the sum of the angles at the “carbanionic” unity, consisting of Si(1), C(3), C(4) and H(3), is 354°. Nevertheless, the tetracoordinate C(3) is a stereogenic centre with the (*R*) configuration due to the Li(1)–C(3) contact; the Li(1)–C(3) distance is 2.254(4) Å. The intramolecular nitrogen–lithium contact [N(1)–Li(1) = 2.185(4) Å] and the intermolecular nitrogen–lithium contact [N(3)–Li(1) = 2.171(4) Å] are equal within the margin of error. As a consequence of the stabilisation effect of silicon centres on vicinal metallated carbon centres (polarisability of the silicon centre in addition to the stabilisation effect by the phenyl substituent), the Si(1)–C(3) bond length [1.817(2) Å] is significantly shorter than the Si(1)–C(10) bond [1.916(2) Å]. Moreover, when the C–C distances in the phenyl ring are compared to a similar (aminomethyl)-(lithiomethyl)benzylsilane that is not lithiated at the benzyl position, the influence of the metallation at C(3) is noticeable. Thus, the C–C distances between the *ipso*- and the two *ortho* carbon centres are longer [C(4)–C(5) = 1.419(4) and C(4)–C(9) = 1.427(3) Å] than the values found previously [1.378(4) and 1.390(4) Å].^[11,12]

The related alkyllithium compound (*R,S*)-2·DABCO crystallised from a toluene/*n*-pentane mixture in the monoclinic crystal system, space group *P*2₁. The asymmetric unit of (*R,S*)-2·DABCO contains one molecule of the alkyllithium as well as one molecule of toluene from the solvent (due to the lack of interactions between the alkyllithium compound and the toluene, the solvent molecule is omitted in Figure 3). In contrast to the TMEDA adduct [(*R,S*)-2]₂·TMEDA, the bidentate DABCO ligand does not bridge two silane units, but coordinates to the lithium centre Li through the nitrogen centre N(2), while the nitrogen centre N(3) remains in a non-coordinating mode [the shortest intermolecular distance N(3)···H(10a) is 2.678(7) Å]. The reason for this is probably the lack of flexibility of the more rigid DABCO, compared to the TMEDA ligand; steric interactions between bridged silane units would be the consequence. The distorted tetrahedral coordination sphere of the lithium centre is built up by one contact to the metallated carbon centre C(3), as well as to O(1) of the meth-

Table 2. Crystal data and structure refinement for [(*R,S*)-2]₂·TMEDA and (*R,S*)-2·DABCO

Compound	[(<i>R,S</i>)-2] ₂ ·TMEDA	(<i>R,S</i>)-2·DABCO
Empirical formula	C ₃₈ H ₆₈ Li ₂ N ₄ O ₂ Si ₂	C ₂₂ H ₃₈ LiN ₃ OSi·C ₆ H ₅ CH ₃
Molecular weight (g·mol ⁻¹)	683.02	487.72
Data collection temperature <i>T</i> (K)	173(2)	173(2)
Wavelength (Å)	0.71073	0.71073
Crystal system	orthorhombic	monoclinic
Space group (no.)	<i>P</i> 2 ₁ 2 ₁ 2 ₁ (19)	<i>P</i> 2 ₁ (4)
<i>a</i> (Å)	13.882(3)	10.1371(19)
<i>b</i> (Å)	17.225(3)	11.711(2)
<i>c</i> (Å)	17.575(4)	13.055(3)
β (°)	—	112.297(3)
Volume (Å ³)	4202.6(15)	1433.9(5)
<i>Z</i>	4	2
Calculated density ρ (g·cm ⁻³)	1.080	1.130
Absorption coefficient μ (mm ⁻¹)	0.119	0.107
<i>F</i> (000)	1496	532
Crystal size [mm ³]	0.20 × 0.20 × 0.20	0.20 × 0.20 × 0.10
Range for data collection 2θ (°)	4.42–50.00	3.38–50.00
Index ranges	–16 ≤ <i>h</i> ≤ 16 –20 ≤ <i>k</i> ≤ 20 –20 ≤ <i>l</i> ≤ 20	–11 ≤ <i>h</i> ≤ 11 –13 ≤ <i>k</i> ≤ 13 –14 ≤ <i>l</i> ≤ 14
Collected reflections	36683	21995
Independent reflections	7407 (<i>R</i> _{int} = 0.1065)	4486 (<i>R</i> _{int} = 0.0867)
Refinement method	full-matrix least-squares on <i>F</i> ²	full-matrix least-squares on <i>F</i> ²
H atom refinement	riding model; H(3) and H(19) refined independently	riding model; H(3) refined independently
Data/restraints/parameters	7407/0/451	4486/1/324
Goodness-of-fit on <i>F</i> ²	1.018	1.062
Final <i>R</i> indices [<i>I</i> > 2σ(<i>I</i>)]	<i>R</i> 1 = 0.0439, <i>wR</i> 2 = 0.1052	<i>R</i> 1 = 0.0685, <i>wR</i> 2 = 0.1544
<i>R</i> indices (all data)	<i>R</i> 1 = 0.0517, <i>wR</i> 2 = 0.1088	<i>R</i> 1 = 0.0711, <i>wR</i> 2 = 0.1560
Absolute structure factor	–0.01(10)	0.2(2)
Largest diff. peak and hole (e·Å ⁻³)	0.380 and –0.276	0.292 and –0.299

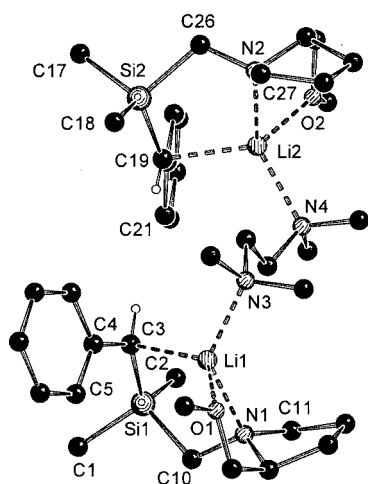


Figure 2. Molecular structure and numbering scheme of compound [(*R,S*)-2]₂·TMEDA in the crystal (Schakal plot);^[10] selected bond lengths (Å) and angles (°): Si(1)–C(3) 1.817(2), Li(1)–C(3) 2.254(4), C(3)–C(4) 1.430(3), N(1)–Li(1) 2.185(4), N(3)–Li(1) 2.171(4), O(1)–Li(1) 1.993(4); C(3)–Si(1)–C(10) 110.19(10), Li(1)–C(3)–Si(1)–C(4) 96.5(2), Si(2)–C(19) 1.809(2), Li(2)–C(19) 2.254(5), C(19)–C(20) 1.437(3), N(2)–Li(2) 2.185(4), N(4)–Li(2) 2.161(4), O(2)–Li(2) 2.013(4), C(19)–Si(2)–C(26) 109.75(12)

oxymethyl substituent and two lithium–nitrogen contacts to nitrogen centres N(1) and N(2) of the SMP substituent and the DABCO ligand. In (*R,S*)-2·DABCO, the metallated car-

bon centre C(3) is also slightly pyramidalised: At the “carbanionic” unit, consisting of Si(1), C(3), C(4) and H(3), a sum of the angles of 358° is found. The tetracoordinate metallated carbon centre C(3), a stereogenic centre due to the Li(1)–C(3) contact, has an (*R*) configuration; the Li(1)–C(3) distance is 2.279(9) Å. The two nitrogen–lithium distances are slightly shorter than in the TMEDA adduct [(*R,S*)-2]₂·TMEDA, but equal within the margin of error [N(1)–Li(1) = 2.138(9) Å (*intramolecular*), N(2)–Li(1) = 2.102(9) Å (*intermolecular*)]. As a consequence of the stabilizing effect of the silicon centre on metallated C(3) (in addition to the stabilisation of the phenyl substituent), the Si–C(3) distance, which amounts to 1.814(5) Å, is significantly shorter than the Si(1)–C(10) distance, which is 1.895(5) Å. In a related non-chiral lithiated benzyl(piperidinomethyl)silane, whose synthesis and crystal structure were reported previously,^[11,12] the corresponding Si(1)–C(3) bond length [1.821(3) Å] is of a similar value, indicating an analogous stabilising effect by the silicon centre of this molecule. The C–C bonds between the *ipso*- and both *ortho* carbon centres [C(4)–C(5) = 1.419(7) and C(4)–C(9) = 1.425(7) Å] are longer than the previously reported values [1.378(4) and 1.390(4) Å].^[11,12]

All three lithiated (aminomethyl)benzylsilanes [(*R,S*)-2, (*R,S*)-2·DABCO and [(*R,S*)-2]₂·TMEDA] are metallated at the benzyl position; the benzylic carbon centre, being the stereogenic metallated carbon centre, has an (*R*) configura-

Table 3. Selected X-ray structural parameters for (*R,S*)-**2**,^[6] [(*R,S*)-**2**]₂·TMEDA (second silane unit in brackets) and (*R,S*)-**2**·DABCO

Compound	(<i>R,S</i>)- 2	[(<i>R,S</i>)- 2] ₂ ·TMEDA	(<i>R,S</i>)- 2 ·DABCO
Absolute configuration at C(3)	(<i>R</i>)	(<i>R</i>) [(<i>R</i>)]	(<i>R</i>)
Sum of the angles at C(3) [°]	360	354 (354)	358
Si(1)–C(3)*/Si–C(3) [Å]	1.797(7)*	1.817(2)* [1.809(2)]	1.814(5)
Li(1)–C(3)*/Li–C(3) [Å]	2.269(14)*	2.254(4)* [2.254(5)]	2.279(9)
Li(1)–N(1)*/Li–N(1) [Å]	2.183(12)*	2.185(4)* [2.185(4)]	2.138(9)
Li(1)–N(3)*/Li–N(2) [Å]	—	2.171(4)* [2.161(4)]	2.102(9)
Li(1)–O(1)*/Li–O [Å]	1.949(13)*	1.993(4)* [2.013(4)]	1.992(9)
C(3)–C(4) [Å]	1.419(9)	1.430(3) [1.437(3)]	1.428(7)
C(4)–C(5) [Å]	1.422(9)	1.419(4) [1.427(4)]	1.419(7)
C(5)–C(6) [Å]	1.412(11)	1.386(4) [1.385(4)]	1.372(7)
C(6)–C(7) [Å]	1.390(12)	1.394(4) [1.350(5)]	1.375(8)
C(7)–C(8) [Å]	1.405(11)	1.370(5) [1.389(6)]	1.387(8)
C(8)–C(9) [Å]	1.369(10)	1.400(4) [1.394(4)]	1.368(8)
C(9)–C(4) [Å]	1.446(9)	1.427(3) [1.405(4)]	1.425(7)
Li(1)–C(3)–Si(1)–C(4)*/Li–C(3)–Si–C(4) [°]	104.1(7)*	96.5(2)* [100.1(3)]	101.6(6)

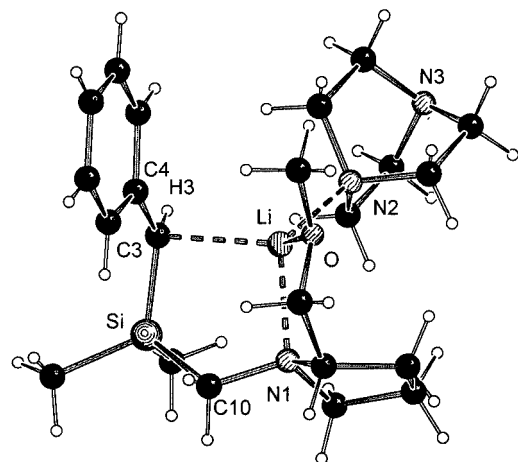


Figure 3. Molecular structure and numbering scheme of compound (*R,S*)-**2**·DABCO in the crystal (Schakal plot)^[10] selected bond lengths (Å) and angles (°): Si–C(3) 1.814(5), Si–C(10) 1.895(5), Li–C(3) 2.279(9), C(3)–C(4) 1.428(7), N(1)–Li 2.138(9), N(2)–Li 2.102(9), O–Li 1.992(9); C(3)–Si(1)–C(10) 109.7(2), Li–C(3)–Si–C(4) 101.6(6)

tion in all three cases. The carbon-lithium distances of the three compounds are equal within the margin of error. This fact underlines — especially in the case of the two intermolecularly coordinated compounds [(*R,S*)-**2**]₂·TMEDA and (*R,S*)-**2**·DABCO — that these compounds do not have the properties of lithium-carbanion pairs. The lithium centre is not separated from the metallated carbon centre, either by the DABCO or by the strongly chelating TMEDA ligand. In the case of compound (*R,S*)-**2**, which is only intramolecularly coordinated by donor centres, the “carbanionic” unit is planar (sum of the angles of 360°), thus the adjoining centres H(3), C(4) and Si are coplanar with C(3). The two externally coordinated compounds [(*R,S*)-**2**]₂·TMEDA and (*R,S*)-**2**·DABCO are slightly pyramidalised at C(3) (sum of the angles of 354° and 358° respectively), although the sums of the angles should not be overvalued. The torsion angles, incorporating the lithium, the silicon, the metallated carbon

and the *ipso* carbon centres, are in the range of 96.5(2)° and 104.1(7)° and demonstrate that the lithium centres are located almost orthogonal to the planes of the “carbanionic” units. Moreover, the periplanar conformation of the C(3)–C(4) bond shows that this “carbanionic” unit is in the same plane as the aromatic ring system. The most important structural parameters of the three alkyl lithium compounds (*R,S*)-**2**,^[6] [(*R,S*)-**2**]₂·TMEDA and (*R,S*)-**2**·DABCO are summarised in Table 3.

An investigation of the molecular structures of (*R,S*)-**2**, (*R,S*)-**2**·DABCO and [(*R,S*)-**2**]₂·TMEDA in solution by low-temperature NMR techniques is not possible due to the poor solubility of the compounds in the essential non-polar solvents at reduced temperatures. At room temperature, no carbon-lithium coupling was observed, although this is not a reliable probe for the carbon-lithium distance.

Quantum-Chemical Studies

Kinetically Controlled Deprotonation

An insight into the deprotonation reaction of (*S*)-**1** with *tert*-butyllithium can be gained by computational methods.^[13] Experimentally, this reaction is effected at very low temperatures (–70 to –90 °C) under kinetically controlled conditions. Under these conditions, the reaction will proceed via the energetically more stable transition state. Two reaction paths are possible, resulting in the formation of the two possible epimers (*R,S*)-**2** and (*S,S*)-**2** (Scheme 1). Each of these reaction paths will be considered separately. With the implication of the complex induced proximity effect (CIPE),^[14] the reaction is believed to start with a pre-coordinated *tert*-butyllithium molecule, whose lithium centre is coordinated by the oxygen and nitrogen atoms of the SMP ligand. From the specific conformation of the Si–C bond in **MIN-1**, the *pro-R* hydrogen atom (H_R) is being abstracted in the deprotonation reaction, proceeding via the transition state **TS-1**, in which the carbon-lithium contact is formed simultaneously with the carbon-hydrogen bond cleavage. The reaction products (metallated silane and *tert*-

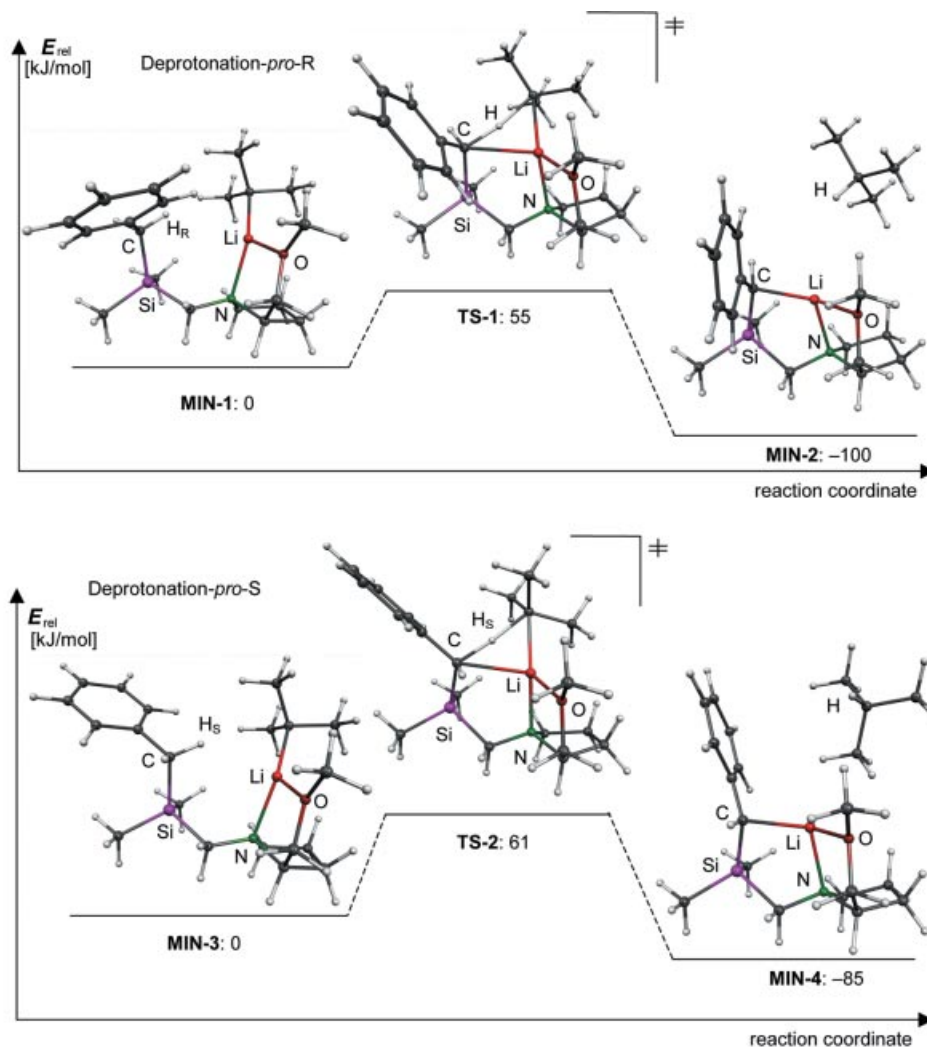


Figure 4. (a) Relative-energy profile of stationary points **MIN-1**, **TS-1** and **MIN-2** for the deprotonation reaction towards the (*R,S*)-epimer, deprotonation-*pro-R*, B3LYP/6–31+G(d); (b) relative-energy profile of stationary points **MIN-3**, **TS-2** and **MIN-4** for the deprotonation reaction towards the (*S,S*)-epimer, deprotonation-*pro-S*, B3LYP/6–31+G(d)

butane) form the stationary point **MIN-2** (Deprotonation-*pro-R*; Scheme 1, Figure 4a, Table 4). The results of this calculation, together with the analogous deprotonation reaction, where the abstraction of the *pro-S* hydrogen atom (H_S) gives the other epimer **MIN-4** (deprotonation-*pro-S*; Scheme 1, Figure 4b, Table 4), are summarised in Table 4.

Table 4. Calculated energies for the stationary points **MIN-1** to **MIN-4**, **TS-1** and **TS-2** of the deprotonation reactions towards the (*R,S*)/(*S,S*)-epimer, B3LYP/6–31+G(d) (ZPVE = Zero-Point Vibrational Energy)

Deprotonation reaction towards (<i>R,S</i>)/(<i>S,S</i>)-epimer		Electronic Energy relative to MIN-1 corrected by ZPVE uncorrected	
	MIN-1	0	0
	TS-1	55	65
	MIN-2	–100	–102
	MIN-3	0	0
	TS-2	61	71
	MIN-4	–85	–88

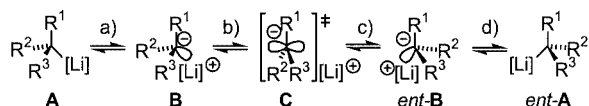
The energies of the two conformers **MIN-1** and **MIN-3** are equal within the margin of error of the DFT method used.^[15] On the reasonable assumption of an equilibrium between **MIN-1** and **MIN-3**, the stereoselectivity of the reaction would be influenced by the difference between the two activation barriers of the potential energy surface of deprotonation-*pro-R* and deprotonation-*pro-S*. This activation barrier for deprotonation-*pro-R* is 6 kJ/mol smaller than the one for the abstraction of the *pro-S* hydrogen atom. This reflects the trend of the kinetically controlled experiment, where the epimer with the (*R*)-configured metallated centre is highly enriched (Scheme 2).^[16] After the deprotonation reaction, two equilibria (epimerisations 1 and 2 in Scheme 1) can influence the distribution of the stereoisomers. This will be examined in the following subsection.

Thermodynamically Controlled Epimerisation — Stability of Configuration

In general, “carbanions” have a low barrier of inversion (they are isoelectronic with tertiary amines). Therefore, un-

substituted systems of this type lose their stereochemical information even at low temperatures. For the racemisation, the following process is assumed (Scheme 5), where the two enantiomeric alkyllithiums **A** and *ent*-**A** are interconverting by separation/fixation of the lithium centre (steps a and d) and the inversion of the configuration via the planar transition state **C** (steps b and c):

The two equilibria (epimerisations 1 and 2 in Scheme 1) can influence the distribution of the stereoisomers after the deprotonation reaction. The situations in non-polar and



Scheme 5. Proposed racemisation process of enantiomerically enriched alkyllithiums: a) separation of the Li fragment; b) and c) inversion of the “carbanion” via a planar transition state; d) fixation of the Li centre

polar solution are, of course, different. While it is reasonable to imply a vacant coordination site at the lithium centre for non-polar solvents (Figure 5a, see also crystal structure in Figure 1), a polar solvent molecule, like diethyl ether, will complete the coordination sphere of the metal centre. This has been demonstrated in the case of amines by the X-ray structural analyses of [(*R,S*)-**2**]₂·TMEDA and (*R,S*)-**2**·DABCO. Thus, the energies of the stationary points of the epimerisation were calculated with a three-coordinate lithium centre (epimerisation 1, Scheme 1; Figure 5a, Table 5) and a four-coordinate lithium centre with an additionally coordinated dimethyl ether and DABCO molecule (epimerisation 2, Scheme 1; Figure 5b and Figure 6, Table 5), to take this into account.

The two reaction products (*R,S*)-**2** and (*S,S*)-**2** (equivalent to **MIN-5** and **MIN-6**, epimerisation 1, Scheme 1; Figure 5a, Table 5) might be involved in an equilibrium process of interconversion. This process, which is undesirable for the kinetically controlled synthesis, is required for the

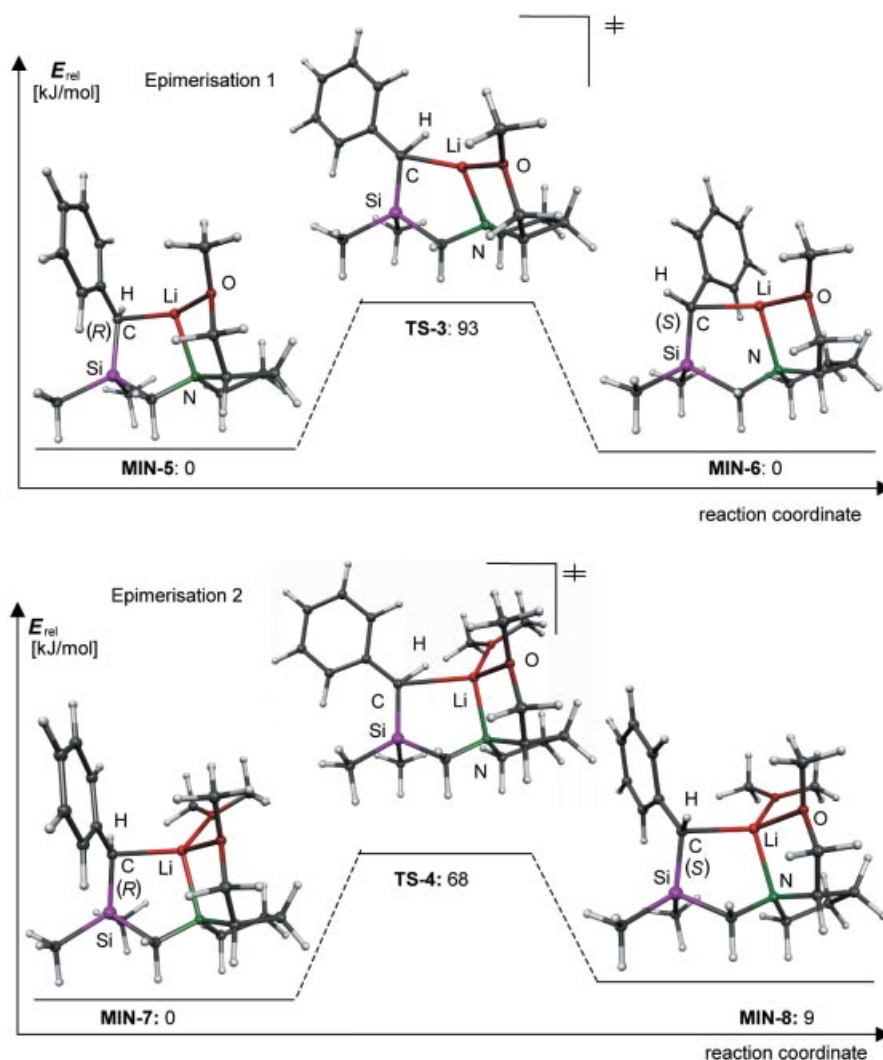
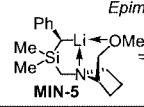
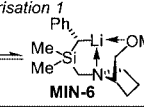
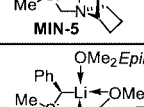
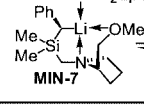
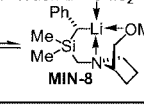
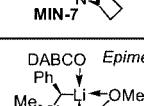
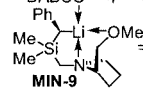
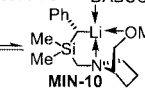
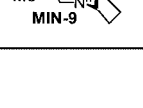
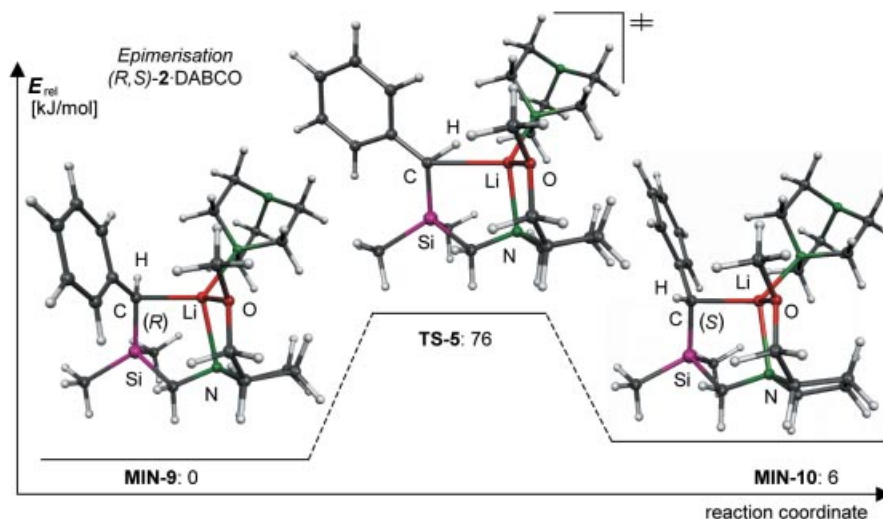


Figure 5. (a) Relative-energy profile of stationary points **MIN-5**, **TS-3** and **MIN-6** for the epimerisation reaction (vacant coordination site) between the (*R,S*)/(*S,S*) epimer, epimerisation 1, B3LYP/6-31+G(d); (b) relative-energy profile of stationary points **MIN-7**, **TS-4** and **MIN-8** for the epimerisation reaction (dimethyl ether molecule coordinated) between the (*R,S*)/(*S,S*) epimer, epimerisation 2, B3LYP/6-31+G(d)

Table 5. Calculated energies for the stationary points **MIN-5** to **MIN-10** and **TS-3** to **TS-5** of the epimerisation reactions between the (*R,S*)/(*S,S*) epimers, B3LYP/6-31+G(d) (ZPVE = Zero-Point Vibrational Energy)

Epimerisation Reaction in non-polar/polar solvent	Electronic Energy relative to MIN-5 / MIN-7 / MIN-9	
	corrected by ZPVE	uncorrected
 MIN-5	0	0
 TS-3	93	95
 MIN-6	0	0
 MIN-7	0	0
 TS-4	68	71
 MIN-8	9	9
 MIN-9	0	0
 TS-5	76	79
 MIN-10	6	6

Figure 6. Relative-energy profile of stationary points **MIN-9**, **TS-5** and **MIN-10** for the epimerisation reaction (DABCO molecule coordinated) between epimers (*R,S*)- and (*S,S*)-2-DABCO, B3LYP/6-31+G(d)

thermodynamically controlled route, where typically a polar solvent is added.

Previous calculations and experimental NMR studies^[5] have shown that the energies for removing the intramolecularly coordinating ligands from the lithium centre and for removing the lithium centre from the metallated carbon centre, are much higher than the energies discussed in Table 4 and 5. Therefore, it is reasonable to exclude a racemisation proceeding via dimeric structures or carbanions.

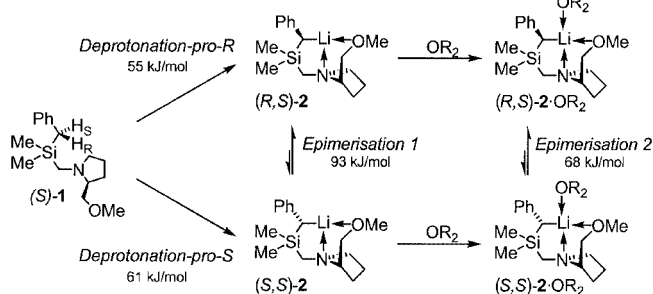
The energy differences of the stationary points **MIN-5**, **TS-3** and **MIN-6** (Figure 5a, Table 5) indicate that an epimerisation process at room temperature is unlikely to occur in a non-polar solvent. In this model system for (*R,S*)-2 in that type of solvent with a vacant coordination site at the lithium centre, the activation barrier on the potential energy surface of epimerisation 1 is 93 kJ/mol.

In the model system for (*R,S*)-2 in a polar solvent with a coordinating dimethyl ether molecule at the lithium centre (epimerisation 2 in Scheme 1), the energy difference between **MIN-7** and **TS-4** is smaller by 25 kJ/mol. Furthermore, in contrast to the described non-polar case, there is an energy difference of 9 kJ/mol between both diastereomeric minimum structures **MIN-7** and **MIN-8**. Concluding these studies, in an ethereal solution, highly diastereomerically enriched (*R,S*)-2 should be obtained by epimerisation at room temperature, while a diastereotopodifferentiating deprotonation without noticeable epimerisation should be possible in non-polar solution (under the described reaction conditions).

For (*R,S*)-2-DABCO, the corresponding calculations have been performed and lead to similar results. [Although a slightly increased inversion barrier is calculated for this

compound, compared to the results with dimethyl ether, the energy difference between both epimers (*R,S*)-2·DABCO and (*S,S*)-2·DABCO decreases slightly]. For this experimentally accessible compound, the more stable epimer (*R,S*)-2·DABCO is the stereoisomer found in the solid state. Thus, experimental structural information can be correlated with the results of selective transformations and the corresponding quantum-chemical investigations.

The experiments with coordinating amine ligands and potentially coordinating ether molecules that have been described in the previous section show very high diastereoselectivities for substitution reactions in non-polar solvents. These results are supported by the quantum-chemical calculations applied on systems of this type (Scheme 6). The poor selectivities of reactions carried out in highly polar solvents, like THF, might not be explained by the calculation of gas-phase structures, since more polar structures are stabilised by the polar solvent environment. Phenomena like this do have an obvious impact on the equilibria and inversion barriers involved and could in an extreme case lead to a change in the reaction mechanism (e.g. orbital control, CIPE control, ionic reaction mechanisms).



Scheme 6. Relevant deprotonation reactions and epimerisation equilibria starting from (*S*)-1 (including the quantum chemically calculated activation barriers for R = Me)

Stereochemical Course

The literature reveals that both retention and inversion of the configuration have been observed for the reactions of lithiated benzylic and related systems with various electrophiles.^[17,3a,3c] In most cases no solid-state structure of the corresponding alkyllithium could be determined to support the absolute configuration of the stereogenic metallated carbon centre. The stereochemical course (inversion of the configuration) of the reaction of our alkyllithiums with the electrophile iodomethane in toluene can be understood on the basis of the solid-state structure of compound (*R,S*)-2·DABCO (crystallised from the same solvent as was used in the substitution reaction with the alkyl iodide) in combination with the computational studies.

The modelling of monomeric (*R,S*)-2·DABCO [B3LYP/6–31+G(d)] indicates that the highest occupied molecular orbital (HOMO) is chiefly located at the metallated carbon centre and the aromatic ring system (Figure 7). It can be deduced from the calculated orbital coefficients that both inversion and retention of the configuration are almost

equally likely to result from electrophilic attack. Only the fact that the site opposite to the lithium centre is sterically accessible to attack by electrophiles makes it possible for (*R,S*)-2·DABCO to react selectively with inversion of configuration at C(3) under kinetic control in non-polar solvents.

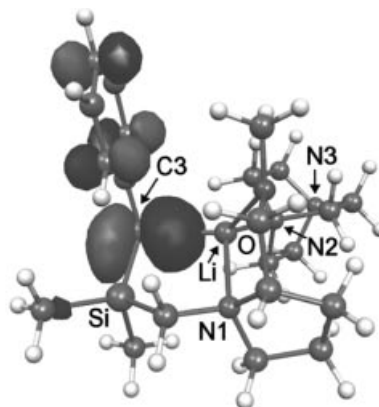


Figure 7. B3LYP/6–31+G(d)-optimised structure of monomeric (*R,S*)-2·DABCO and visualisation of the highest occupied molecular orbital (HOMO) (Molekel plot;^[18] numbering scheme adopted from Figure 3)

Outlook

In a recent review article by Basu and Thayumanavan, the following quote on the main challenges in this research field can be found: “We believe that the first of these challenges is the development of a systematic structure-function relationship for the stereochemical behaviour of organolithium compounds. There have only been a few instances in which structural information about organolithium aggregates have been used as the starting point for the design of stereoselective lithiation/substitution sequences.”^[2a]

It is hoped that the correlation of experimental data, like stereoselectivities and the stereochemical pathways — especially results from solid-state structural analyses — will lead to a deeper understanding of the transformations of (highly diastereomerically enriched) alkyllithium compounds. It must always be of general interest to determine whether the results of such investigations may be of use in understanding the reaction pathways of alkyllithium systems, or if studies of systems like (*R,S*)-2 and its derivatives are too specialised to set up common rules for the stereochemistry of this class of compounds.^[19]

Experimental Section

Experimental Procedures: All reactions were carried out under an argon atmosphere using Schlenk tubes that had been flame-dried in vacuo. The solvents, including the NMR solvents, were dried according to common procedures. All NMR spectra were measured on a Bruker DRX-300 NMR spectrometer. Assignment of the signals was supported by DEPT135 and C,H-COSY experiments and

the relative intensities of the resonance signals. Crystal structure determination of [(*R,S*)-2]₂·TMEDA: Stoe IPDS diffractometer (Stoe & Cie GmbH); data collection: Expose (Stoe & Cie, 1997); cell determination and refinement: Cell (Stoe & Cie, 1997); integration: Integrate (Stoe & Cie, 1999); numerical absorption correction: Faceit (Stoe & Cie, 1997). Crystal structure determination of (*R,S*)-2·DABCO: Bruker APEX-CCD (D8 three-circle goniometer) (Bruker AXS); data collection, cell determination and refinement: Smart version 5.622 (Bruker AXS, 2001); integration: SaintPlus version 6.02 (Bruker AXS, 1999); empirical absorption correction: Sadabs version 2.01 (Bruker AXS, 1999). The determination of the absolute configurations at the metallated stereogenic carbon centres of both compounds is unambiguous due to the fixed (*S*) configuration at the SMP substituent; for the achieved crystal quality of (*R,S*)-2·DABCO, the lack of a heavier atom than silicon does not allow a refinement of the absolute structure factor (Flack parameter) better than 0.2(2), indicating yet the overall refinement of the correct stereoisomer. The crystals of both compounds were mounted at −100 °C (N₂ stream), using the X-TEMP 2 device.^[20] Both structures were solved applying direct and Fourier methods, using SHELXS-90^[21] and SHELXL-97.^[22] CCDC-210324 {[(*R,S*)-2]₂·TMEDA} and CCDC-210325 [(*R,S*)-2·DABCO] contain the supplementary crystallographic data for this paper. These data can be obtained free of charge at www.ccdc.cam.ac.uk/conts/retrieving.html [or from the Cambridge Crystallographic Data Centre, 12, Union Road, Cambridge CB2 1EZ, UK; Fax: (internat.) +44-1223/336-0333; E-mail: deposit@ccdc.cam.ac.uk].

Computational Methods: All calculations were carried out on gas-phase structures. Structure optimisations at the B3LYP/6-31+G(d) level were performed using GAUSSIAN 98.^[13] The basis for the starting structures were the coordinates of the X-ray structural analyses of (*R,S*)-2 and (*R,S*)-2·DABCO; different starting conformers [C(3)–C(4) bond] were also investigated. Selected bond lengths [Å] and angles [°] of the optimised structure (*R,S*)-2·DABCO: Si–C(3) 1.832, Si–C(10) 1.941, Li–C(3) 2.211, Li–N(1) 2.206, Li–N(2) 2.170, Li–O 2.047, C(3)–C(4) 1.451, C(3)–Si–C(10) 108.5. For all transition states, only one imaginary frequency was found. For the deprotonation reactions, the vibrational modes corresponding to the imaginary frequency were in the direction of the C(3)–H bond dissociation. For the epimerisation reactions, the vibrational modes corresponding to the imaginary frequency were in the direction of the inversion of the configuration at C(3). IRC calculations (intrinsic reaction coordinate) were performed at the HF/3-21G level of theory.

[(*R,S*)-2]₂·TMEDA: A solution of (aminomethyl)benzylsilane [(*S*)-1; 450 mg, 1.62 mmol] and TMEDA (94.0 mg, 810 μmol) in *n*-pentane was combined with 950 μL (1.62 mmol) of a solution of *t*BuLi in *n*-pentane (1.7 M) at −90 °C. Upon warming to room temp. the lithium compound [(*R,S*)-2]₂·TMEDA was obtained as a microcrystalline orange powder. Whilst stirring at room temp., toluene was added dropwise until a solution was obtained. The yellow solution was kept at −30 °C. After 14 days at −30 °C [(*R,S*)-2]₂·TMEDA was obtained as orange-coloured single-crystals suitable for X-ray structural analysis (yield: 509 mg, 745 μmol, 92%). ¹H NMR (300.1 MHz, C₆D₅CD₃): δ = 0.27 (s, 6 H, SiCH₃), 0.31 (s, 6 H, SiCH₃), 1.29–1.58 (m, 8 H, CH₂), 1.82 [br, 2 H, SiC(H)Li], 1.89–2.04 (m, 18 H, NCH₃, NCH₂C, NCH), 2.11–2.28 (m, 4 H, NCH₂CH₂N), 1.45, 2.56 (AB-System, ²J_{A,B} = 14.3 Hz, 2 H, SiCH₂N), 2.64 (ABX-System, unresolved, 2 H, CH₂O), 2.67 (s, 6 H, OCH₃), 3.03–3.19 (m, 2 H, CH₂), 3.24 (ABX-System, unresolved, 2 H, CH₂O), 6.19–6.23 (m, 2 H, aromat. H), 6.64–6.67 (m, 4 H, aromat. H), 6.90–6.97 (m, 4 H, aromat. H) ppm. ⁷Li{¹H}

NMR (116.6 MHz, C₆D₅CD₃): δ = 0.46 ppm. ¹³C{¹H} NMR (75.5 MHz, C₆D₅CD₃): δ = −1.6 (2C, SiCH₃), 0.9 (2C, SiCH₃), 22.1 (2C, CH₂), 26.6 (2C, CH₂), 36.7 (2C) [SiC(H)Li], 45.8 (4C, NCH₃), 47.8 (2C, SiCH₂N), 57.1 (2C, NCH₂CH₂N), 57.8 (2C, NCH₂C), 58.7 (2C, OCH₃), 67.3 (2C, NCH), 70.8 (2C, CH₂O), 108.6 (2C, C-p), 119.9 (4C, C-m or C-o), 137.4 (4C, C-o or C-m), 157.3 (2C, C-i) ppm. ²⁹Si{¹H} NMR (59.6 MHz, C₆D₅CD₃): δ = −13.2 ppm.

(*R,S*)-2·DABCO: A solution of (aminomethyl)benzylsilane [(*S*)-1; 440 mg, 1.59 mmol] and DABCO (179 mg, 1.59 mmol) in *n*-pentane was combined with 935 μL (1.59 mmol) of a solution of *t*BuLi in *n*-pentane (1.7 M) at −90 °C. Upon warming to room temp. lithium compound (*R,S*)-2·DABCO was obtained as a microcrystalline yellow powder. Whilst stirring at room temp., toluene was added dropwise until a solution was obtained. The yellow solution was kept at −30 °C. After 21 days at −30 °C (*R,S*)-2·DABCO was obtained as yellow single-crystals suitable for X-ray structural analysis (yield: 744 mg, 1.53 mmol, 96%). ¹H NMR (300.1 MHz, C₆D₅CD₃): δ = 0.24 (s, 3 H, SiCH₃), 0.41 (s, 3 H, SiCH₃), 1.19–1.41 (m, 4 H, CH₂), 1.43, 2.60 (AB-System, ²J_{A,B} = 14.2 Hz, 2 H, SiCH₂N), 1.78 [br, 1 H, SiC(H)Li], 1.85–2.07 (m, 2 H, NCH, NCH₂), 2.42 (s, 12 H, NCH₂CH₂N), 2.60 (s, 3 H, OCH₃), 2.97–3.00 (ABX-System, unresolved, 1 H, CH₂O), 2.97–3.06 (m, 1 H, NCH₂), 3.33–3.39 (ABX-System, unresolved, 1 H, CH₂O), 6.31–6.36 (m, 1 H, aromat. H), 6.69–6.72 (m, 2 H, aromat. H), 7.10–7.19 (m, 2 H, aromat. H) ppm. ⁷Li{¹H} NMR (116.6 MHz, C₆D₅CD₃): δ = 0.45 ppm. ¹³C{¹H} NMR (75.5 MHz, C₆D₅CD₃): δ = −2.2 (br., SiCH₃), 0.7 (SiCH₃), 22.8 (CH₂), 26.6 (CH₂), 34.5 [SiC(H)Li], 47.8 (6C, NCH₂CH₂N), 48.1 (SiCH₂N), 57.9 (NCH₂), 58.8 (OCH₃), 67.7 (NCH), 70.3 (CH₂O), 108.6 (C-p), 124.3 (2C, C-m or C-o), 128.9 (2C, C-o or C-m), 157.5 (C-i) ppm. ²⁹Si{¹H} NMR (59.6 MHz, C₆D₅CD₃): δ = −13.6 ppm.

Absolute electronic energies [B3LYP/6-31+G(d)] including ZPVE correction (uncorrected values in brackets): **MIN-1** −1210.329989 (−1210.85396686), **MIN-2** −1210.367902 (−1210.89273147), **TS-1** −1210.309066 (−1210.82931116), **MIN-3** −1210.330119 (−1210.85397884), **MIN-4** −1210.362321 (−1210.88757733), **TS-2** −1210.306980 (−1210.82688289), **MIN-5** −1052.035771 (−1052.42846659), **MIN-6** −1052.035924 (−1052.42849744), **TS-3** −1052.000391 (−1052.39218728), **MIN-7** −1207.002773 (−1207.47727275), **MIN-8** −1206.999447 (−1207.47375891), **TS-4** −1206.973602 (−1207.44687856), **MIN-9** −1397.204510 (1397.78271366), **MIN-10** −1397.202535 (−1397.78059515), **TS-5** −1397.175908 (−1397.75282437).

Acknowledgments

We are grateful to the Institut für Anorganische Chemie der Universität Würzburg, the Deutsche Forschungsgemeinschaft (DFG), the Sonderforschungsbereich 347, the Graduiertenkolleg 690, and the Fonds der Chemischen Industrie (FCI) for financial support. D. S. and K. W. thank the FCI for the grant of two scholarships. Furthermore we acknowledge Wacker-Chemie GmbH for providing us with special chemicals.

^[1] Remark: In general, we speak of *enantiomerically enriched* metal alkyls when we focus our interest on the stereogenic metallated carbon centre, whereas these molecules are almost always *diastereomerically enriched* metal alkyls, due to the presence of more stereogenic centres than only the metallated one.

^[2] ^[2a] A. Basu, S. Thayumanavan, *Angew. Chem. Int. Ed.* **2002**, *41*, 716, and literature cited therein. ^[2b] D. Hoppe, T. Hense,

- Angew. Chem. Int. Ed. Engl.* **1997**, *36*, 2282, and literature cited therein.
- [3] For examples see: [3a] O. Stratmann, B. Kaiser, R. Fröhlich, O. Meyer, D. Hoppe, *Chem. Eur. J.* **2001**, *7*, 423. [3b] P. Beak, D. R. Anderson, M. D. Curtis, J. M. Laumer, D. J. Pippel, G. A. Weisenburger, *Acc. Chem. Res.* **2000**, *33*, 715. [3c] G. A. Weisenburger, N. C. Faibish, D. J. Pippel, P. Beak, *J. Am. Chem. Soc.* **1999**, *121*, 9522. [3d] D. J. Pippel, G. A. Weisenburger, S. R. Wilson, P. Beak, *Angew. Chem. Int. Ed.* **1998**, *37*, 2522. [3e] D. Hoppe, B. Kaiser, O. Stratmann, R. Fröhlich, *Angew. Chem. Int. Ed. Engl.* **1997**, *36*, 2784. [3f] H. Ahlbrecht, J. Harbach, R. W. Hoffmann, T. Ruhland, *Liebigs Ann.* **1995**, 211. [3g] G. Boche, M. Marsch, J. Harbach, K. Harms, B. Ledig, F. Schubert, J. C. W. Lohrenz, H. Ahlbrecht, *Chem. Ber.* **1993**, *126*, 1887. [3h] R. I. Papasergio, B. W. Skelton, P. Twiss, A. H. White, C. L. Raston, *J. Chem. Soc., Dalton Trans.* **1990**, 1161.
- [4] [4a] T. H. Chan, P. Pellon, *J. Am. Chem. Soc.* **1989**, *111*, 8737. [4b] T. H. Chan, S. Lamothe, *Tetrahedron Lett.* **1991**, *32*, 1847. [4c] T. H. Chan, K. T. Nwe, *J. Org. Chem.* **1992**, *57*, 6107.
- [5] [5a] G. Fraenkel, J. H. Duncan, K. Martin, J. Wang, *J. Am. Chem. Soc.* **1999**, *121*, 10538. [5b] G. Fraenkel, K. Martin, *J. Am. Chem. Soc.* **1995**, *117*, 10336.
- [6] C. Strohmman, K. Lehmen, K. Wild, D. Schildbach, *Organometallics* **2002**, *21*, 3079.
- [7] M. Marsch, K. Harms, O. Zschage, D. Hoppe, G. Boche, *Angew. Chem. Int. Ed. Engl.* **1991**, *30*, 321.
- [8] I. Hoppe, M. Marsch, K. Harms, G. Boche, D. Hoppe, *Angew. Chem. Int. Ed. Engl.* **1995**, *34*, 2158.
- [9] H. Ahlbrecht, G. Boche, K. Harms, M. Marsch, H. Sommer, *Chem. Ber.* **1990**, *123*, 1853.
- [10] E. Keller, Schakal 99, University of Freiburg (Germany): Freiburg 1999.
- [11] D. Schildbach, *Doctoral Thesis*, University of Würzburg **2002**.
- [12] C. Strohmman, K. Lehmen, A. Ludwig, D. Schildbach, *Organometallics* **2001**, *20*, 4138.
- [13] Gaussian 98, Revision A.9, M. J. Frisch, G. W. Trucks, H. B. Schlegel, G. E. Scuseria, M. A. Robb, J. R. Cheeseman, V. G. Zakrzewski, J. A. Montgomery, Jr., R. E. Stratmann, J. C. Burant, S. Dapprich, J. M. Millam, A. D. Daniels, K. N. Kudin, M. C. Strain, O. Farkas, J. Tomasi, V. Barone, M. Cossi, R. Cammi, B. Mennucci, C. Pomelli, C. Adamo, S. Clifford, J. Ochterski, G. A. Petersson, P. Y. Ayala, Q. Cui, K. Morokuma, D. K. Malick, A. D. Rabuck, K. Raghavachari, J. B. Foresman, J. Cioslowski, J. V. Ortiz, A. G. Baboul, B. B. Stefanov, G. Liu, A. Liashenko, P. Piskorz, I. Komaromi, R. Gomperts, R. L. Martin, D. J. Fox, T. Keith, M. A. Al-Laham, C. Y. Peng, A. Nanayakkara, M. Challacombe, P. M. W. Gill, B. Johnson, W. Chen, M. W. Wong, J. L. Andres, C. Gonzalez, M. Head-Gordon, E. S. Replogle, J. A. Pople, Gaussian, Inc., Pittsburgh PA, 1998.
- [14] F. Haefner, P. Brandt, R. E. Gawley, *Org. Lett.* **2002**, *4*, 2101.
- [15] All corrected and uncorrected electronic energies are given relative to MIN-1.
- [16] At this point, the influence of the indispensable correction of all optimised structures by the *zero-point vibrational energy* (ZPVE) becomes obvious, since it decreases the absolute energies of the transition states more than those the minimum structures. This, and the computational method itself, significantly affect the electronic part of the activation energy. Thus, conclusions, deriving from too accurate comparisons of calculations with experimental data have to be drawn very carefully but can be found in the literature time and time again.
- [17] For examples see: [17a] F. Marr, R. Fröhlich, D. Hoppe, *Org. Lett.* **1999**, *1*, 2081. [17b] N. C. Faibish, Y. S. Park, S. Lee, P. Beak, *J. Am. Chem. Soc.* **1997**, *119*, 11561. [17c] M. D. Curtis, P. Beak, *J. Org. Chem.* **1999**, *64*, 2996. [17d] F. Hammerschmidt, A. Hanninger, B. C. Simov, H. Völlenkle, A. Werner, *Eur. J. Org. Chem.* **1999**, 3511.
- [18] S. Portmann, Molekel, Version 4.1.win-32, ETH Zürich (Switzerland), Zürich 2001.
- [19] C. Strohmman, B. C. Abele, K. Lehmen, F. Villafañe, L. Sierra, S. Martín-Barrios, D. Schildbach, *J. Organomet. Chem.* **2002**, *661*, 149.
- [20] T. Kottke, D. Stalke, *J. Appl. Cryst.* **1993**, *26*, 615.
- [21] G. M. Sheldrick, SHELXS-90, *A Program for the Solution of Crystal Structures*, Universität Göttingen 1990.
- [22] G. M. Sheldrick, SHELXL-97, *A Program for Crystal Structure Refinement*, Universität Göttingen 1997.

Received May 29, 2003